

Effect of User Mobility on the Performance of Device-to-Device Networks with Distributed Caching

Shankar Krishnan and Harpreet S. Dhillon

Abstract

A distributed caching device-to-device (D2D) network is considered, where a user's file of interest is cached as several portions in the storage of other devices in the network and obtained successively through D2D communication. A higher likelihood of dominant interferers for the file portions cached farther away from the user's location presents a *bottleneck* in obtaining the entire file. With device locations modeled as a Poisson Point Process (PPP), we derive new analytical expressions for the coverage probability and *local delay* of the file cached farther from the typical device in a 2-file distributed caching network as a function of the distance v moved by the user from its initial location. For a uniform caching network with a maximum storage of one file portion per device, we show that mobility significantly improves network performance.

Index Terms

Distributed caching, D2D network, mobility, stochastic geometry, Poisson point process, coverage probability, local delay.

I. INTRODUCTION

Caching popular content on the user devices and delivering it asynchronously to other proximate devices via D2D communication helps offload traffic from cellular network [1]. However, with the increasing popularity of ultra-HD videos (larger file sizes), it will become increasingly difficult to cache the entire file of interest in a single mobile device. Even though storage costs

The authors are with Wireless@VT, Department of ECE, Virginia Tech, Blacksburg, VA, USA. Email: {kshank93, hdhillon}@vt.edu.

are decreasing, only a small fraction of user device's memory may be allotted for caching files. This has led to the consideration of *distributed storage* regime [2], where the file of interest is stored as multiple portions among different devices in the network. While this has mostly been explored from the information theoretic perspective, e.g., see [3], we study this problem from wireless communications perspective. In particular, for the file portions cached geographically farther from the typical user's location, there is a likelihood of having dominant interferers closer than the serving device, which present a *bottleneck* in the reception of the complete file [4]. In this paper, we use tools from stochastic geometry to quantify the effect of user mobility on this bottleneck in terms of both coverage probability and *local delay* [5]. More details are provided next.

Prior work: There exist some prior works in the literature focusing on user mobility in cache-enabled networks which can be broadly classified into two main categories. The first line of work deals with a *storage allocation problem*, where content is proactively stored in the memory of small cells or devices along the user's mobility pattern to support seamless connectivity. The authors in [6] consider a distributed storage system, which stores different *chunks* of a movie requested by a moving user in different Wi-Fi APs to support live streaming of the movie. An optimal storage allocation scheme which minimizes the access probability of files from the macro base-station in a coded cache-enabled network when the user mobility is modeled as discrete-time Markov model is dealt in [7]. The second line of work deals with studying key metrics such as coverage probability or local delay of a moving user in *random* wireless network. The authors in [5] studied finite mobility in Poisson networks; derived various bounds of local delay for different mobility and transmission models and showed that user mobility helps reduce the local delay. While studying the impact of mobility of transmitters in a multicast D2D network, [8] showed that mobility increases the mean number of *covered* receivers. In this work, we build upon this observation and show that mobility increases the chance of a user being closer to a device that has cached its file of interest in a distributed storage scenario. The key difference behind our and these existing works is that we provide new analytical results on these key metrics capturing the user's local neighborhood as it moves around in a distributed caching network. Further details are provided next.

Contributions: Assuming a storage capacity of one file portion per device, we study the effect of user mobility on the coverage probability and average local delay experienced by a typical

device while obtaining cached file portions. Specifically, we study a 2-file distributed caching system, where a typical user successfully receives one file portion at its initial location and receives the other file portion at its next location, which is assumed to be distance $v \geq 0$ away. Modeling the device locations as a PPP, we first derive distance distributions for receiving the second file portion (termed *farther* file portion) at the second location. The exact analysis at the second location is not straightforward and requires the knowledge of the *local neighborhood* as observed at the first location. After carefully incorporating this information in the form of asymmetric *exclusion zone* with respect to the second location, we derive tractable expressions for the coverage probability and local delay of receiving the farther cached file portion (the one that was not received at the first location) for different levels of mobility. Our results concretely demonstrate that coverage probability at the second location increases with user mobility and asymptotically approaches an *independent* scenario, where the coverage probability of a file portion is independent of its geographical location in the network. Lower local delays also result with user mobility.

II. SYSTEM MODEL

System Setup: Device locations are modeled as a homogeneous PPP Φ with intensity λ . We consider a 2-file distributed caching system where each device has either file A or file B cached independently with probabilities $p_A = p$ and $p_B = 1 - p$. Here file A and B correspond to two portions of a larger file requested by the *typical* device. Independent thinning of the original PPP Φ results in two independent PPPs, Φ_A for file A and Φ_B for file B. Conditioned on the serving link, each interferer is assumed to be active independently with probability q . This activity factor captures the fact that all the devices in the network may not always be active.

Channel Model: For the wireless channels, we assume distance-dependent power-law pathloss with exponent α and Rayleigh fading. For a typical user located at the origin, the power received at the user from a device $x \in \Phi$ is $P = P_t h_x \|x\|^{-\alpha}$, where P_t is the transmit power, $h_x \sim \exp(1)$ models Rayleigh fading, and $\alpha > 2$ is the pathloss exponent. To define the interference power, we need an additional binary random variable t_y , which takes value 1 with probability q and 0 otherwise. For this setup, the received signal to interference ratio (SIR) at the typical device can

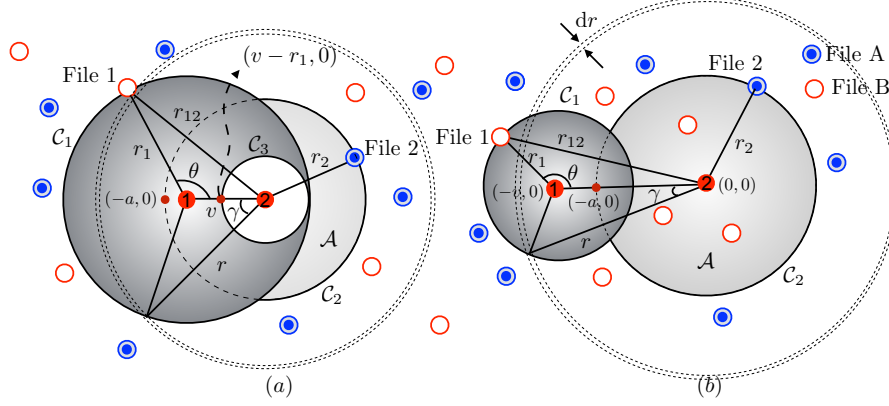


Fig. 1. System model. (a) Scenario 1 ($v < r_1$) and (b) Scenario 2 ($v > r_1$). A user at location 1 $(-v, 0)$ receives file 1 and moves a distance v to location 2 $(0, 0)$, where it receives file 2. Subcase \mathcal{Y} is shown (File B is File 1).

be expressed as

$$\text{SIR} = \frac{P_t h_x \|x\|^{-\alpha}}{\sum_{y \in \Phi \setminus \{x\}} t_y P_t h_y \|y\|^{-\alpha}} = \frac{h_x \|x\|^{-\alpha}}{\sum_{y \in \Phi \setminus \{x\}} t_y h_y \|y\|^{-\alpha}}. \quad (1)$$

We consider out-of-band D2D due to which the interference from the cellular network does not show up in the received SIR. Quite reasonably, the network is assumed to be interference limited, as a result of which the thermal noise is ignored in comparison to the interference power.

III. EFFECT OF USER MOBILITY ON COVERAGE

A user initially located at $(-v, 0)$, termed *location 1*, connects to its closest device and successfully receives the file portion cached by that device (can be file A or B). This user then moves distance v to *location 2* (taken to be the origin) and receives the other file portion from the closest device that has the other file portion in its cache. Our goal is to study the coverage probability at *location 2* as a function of v ($v = 0$ models *static* case studied in [4]). We label the closest file portion cached to the user at location 1 (can be file A or B) as *file 1* and the other file portion as *file 2*. Fig. 1 depicts this system setup with R_1 and R_2 denoting the distances of the user at locations 1 and 2 to the closest device with file 1 and file 2, respectively (r_1, r_2 denote realizations of R_1, R_2). Also let us define two circles: \mathcal{C}_1 centered at location 1 with radius r_1 and \mathcal{C}_2 centered at location 2 with radius r_2 . When user moves a distance v from location 1 to 2, one of the following three cases arises: (i) *Case 1*: Disjoint circles ($v \geq r_1 + r_2$),

(ii) *Case 2*: Intersecting circles ($r_2 - r_1 < v < r_1 + r_2$), and (iii) *Case 3*: Engulfed circles ($v \leq r_2 - r_1$). Following intermediate result will be useful for our analysis.

Definition 1. Consider two partially-overlapping circles with radii r_1 and r_2 with centers separated by distance v , where $r_2 - r_1 < v < r_1 + r_2$, as shown in Fig. 1. The lightly shaded region \mathcal{A} is called a *lune* and its area is [9, Equation (12.76)]

$$\begin{aligned} \mathcal{A}_{\text{lune}} = & \pi r_2^2 + \frac{1}{2} \sqrt{[(r_1 + v)^2 - r_2^2][r_2^2 - (r_1 - v)^2]} \\ & - r_1^2 \cos^{-1} \left(\frac{r_1^2 + v^2 - r_2^2}{2vr_1} \right) - r_2^2 \cos^{-1} \left(\frac{r_2^2 + v^2 - r_1^2}{2vr_2} \right). \end{aligned}$$

A. Distance distribution

As defined before, R_1 is the random variable denoting the distance of the closest file portion (file 1) from location 1. It is by definition the distance from location 1 to the closest point of a PPP with intensity λ . Its distribution can be found from the null probability of a PPP as $f_{R_1}(r_1) = 2\pi\lambda r_1 e^{-\lambda\pi r_1^2}$ [10]. For the system setup studied in this paper, there exist two possible subcases: (i) \mathcal{X} : File A is file 1 (occurs with probability p_A) and (ii) \mathcal{Y} : File B is file 1 (occurs with probability p_B). The subcase \mathcal{Y} is depicted in Fig. 1.

As there exists no device cached with either file portion within a distance r_1 from location 1, \mathcal{C}_1 can be interpreted as an *exclusion zone* in the interference field. Conditioned on a certain file portion located at a distance r_1 , the distribution of R_2 is hence dictated by the presence of no devices caching the other file portion in $\mathcal{C}_2 \setminus \mathcal{C}_1$. In Fig. 1, the lightly shaded region \mathcal{A} represents $\mathcal{C}_2 \setminus \mathcal{C}_1$, which depends on the distance v moved by the user between location 1 and 2. As per the definition of the three cases, \mathcal{A} is represented by the entire circle \mathcal{C}_2 in case of disjoint circles (case 1), a *lune* in case of intersecting circles (case 2) or an annular region between circles \mathcal{C}_1 and \mathcal{C}_2 in case of engulfed circles (case 3). The area of \mathcal{A} is mathematically expressed in Lemma 1.

Before stating Lemma 1, it is worth defining two scenarios: termed *scenarios 1* and 2, based on the distance v moved by the user from location 1 to 2. In scenario 1, distance v moved by the user is smaller than the serving distance at location 1 i.e. $v < r_1$. As a result, the user is still inside circle \mathcal{C}_1 (Fig.1 (a)) and hence no device can lie within a distance $r_1 - v$ from location 2. Thus, the closest device with file 2 is located atleast a distance of $r_1 - v$ away from location

2 ($r_2 \geq r_1 - v$). In scenario 2, the user moves a larger distance ($v > r_1$), as a result of which the user moves out of the circle \mathcal{C}_1 (Fig.1 (b)). Hence there exists no such condition for the serving distance R_2 of file 2 in scenario 2. The above mathematical conditions for R_2 based on the two scenarios are handled appropriately by defining $z_1 = \max(0, r_1 - v)$ as its lower limit. Also let us define a circle \mathcal{C}_3 centered at location 2 and a radius of z_1 , which will be used later in the analysis. It is to be noted that \mathcal{C}_3 converges to a point for scenario 2 ($v > r_1$) and hence not shown in the corresponding figure. The conditional distribution of R_2 is now derived next in Lemma 1.

Lemma 1. *For a given v , the conditional distribution of distance R_2 from location 2, conditioned on r_1 is*

$$f_{R_2|R_1}(r_2|r_1) = \frac{d}{dr_2}(1 - e^{-\lambda_2|\mathcal{A}|}), \quad r_2 \geq \max(0, r_1 - v)$$

$$|\mathcal{A}| = \begin{cases} \pi r_2^2, & \max(0, r_1 - v) \leq r_2 \leq |v - r_1| \\ \mathcal{A}_{\text{lune}}, & |v - r_1| < r_2 < v + r_1 \\ \pi(r_2^2 - r_1^2), & r_2 \geq v + r_1 \end{cases}$$

where $\lambda_2 = p_A \lambda$ with probability p_A and $p_B \lambda$ otherwise.

Proof: Conditioned on the presence of no device caching the other file portion (PPP of intensity λ_2) within a distance r_1 from location 1 (or equivalently in \mathcal{C}_1), the complementary CDF of R_2 is given by

$$\bar{F}_{R_2|R_1}(r_2|r_1) = \mathbb{P}(N(|\mathcal{C}_2|) = 0 | N(|\mathcal{C}_1|) = 0) = \mathbb{P}(N(|\mathcal{C}_2 \setminus \mathcal{C}_1|) = 0) \stackrel{(a)}{=} \exp(-\lambda_2|\mathcal{A}|)$$

where $|\cdot|$ denotes the area, $N(\cdot)$ is the number of files of other type in the specified area, and (a) results from the null probability of a PPP with intensity λ_2 . The result now follows by differentiating the CDF and using appropriate values for the area of \mathcal{A} . ■

B. Coverage probability of file 2

A user is said to be in coverage of a certain file portion if the received SIR at that user from a device caching that file portion is greater than a coding and modulation specific threshold T i.e. coverage probability $P_c = \mathbb{P}(\text{SIR} > T)$. For the coverage probability analysis of file 2, we just focus on subcase \mathcal{Y} (file B is file 1). Result for subcase \mathcal{X} will follow immediately by

swapping the variables. The total coverage probability of obtaining file 2 is derived by applying total probability theorem to the two subcases as $P_{c_2} = p_A P_{c_2}^{(\mathcal{X})} + p_B P_{c_2}^{(\mathcal{Y})}$, where $P_{c_2}^{(\mathcal{X})}$ and $P_{c_2}^{(\mathcal{Y})}$ denote the conditional coverage probability of obtaining file 2 in subcases \mathcal{X} and \mathcal{Y} , respectively. Conditioned on R_1 and R_2 , the coverage probability $P_{c_2}^{(\mathcal{Y})}$ can be determined by dividing the total interference field into three regions as described below.

I_1 : Interference experienced at location 2 due to the transmission of the device $x \in \Phi_B$ (has file B) that was the *serving* device for location 1. As shown in Fig. 1, this device is at distance r_{12} from location 2. The interference power is

$$I_1 = t_x h_x r_{12}^{-\alpha}. \quad (2)$$

I_2 : Interference at location 2 from all devices with file B except the singleton $\{x\}$ at distance r_{12} . This interference field is essentially Φ_B with an *asymmetric* exclusion zone \mathcal{C}_1 created by the exclusion of $\{x\}$. The interference power is

$$I_2 = \sum_{y \in \Phi_B \setminus \mathcal{C}_1} t_y h_y \|y\|^{-\alpha}. \quad (3)$$

I_3 : Interference at location 2 from all devices with file A except the serving device from Φ_A at distance r_2 . As there exists no device with file A in \mathcal{C}_1 , this interference is equivalent to considering interference from Φ_A outside *exclusion zone* $\mathcal{C}_1 \cup \mathcal{C}_2$. The interference power is

$$I_3 = \sum_{z \in \Phi_A \setminus (\mathcal{C}_1 \cup \mathcal{C}_2)} t_z h_z \|z\|^{-\alpha}. \quad (4)$$

Due to the Rayleigh fading assumption, coverage probability in general can be expressed in terms of the Laplace transform of the interference power distribution [10], [11]. Due to the independence of the three interference terms defined above, the Laplace transform of the distribution of total interference can be expressed as the product of the Laplace transforms of the three terms. Using this, the coverage probability of obtaining file 2 in subcase \mathcal{Y} can be expressed as follows.

Theorem 1. *The coverage probability of obtaining file 2 at location 2 in a PPP of intensity λ for subcase \mathcal{Y} is*

$$\begin{aligned} P_{c_2}^{(\mathcal{Y})} = & \int_0^\infty \int_{z_1}^\infty \int_0^\pi \mathcal{L}_{I_1|R_1, \Theta}(Tr_2^\alpha | r_1, \theta) \mathcal{L}_{I_2|R_1}(Tr_2^\alpha | r_1) \\ & \mathcal{L}_{I_3|R_1, R_2}(Tr_2^\alpha | r_1, r_2) f_{R_2|R_1}(r_2 | r_1) f_{R_1}(r_1) f_\Theta(\theta) d\theta dr_2 dr_1 \end{aligned}$$

where the conditional Laplace transforms of I_1 , I_2 and I_3 are derived below in Lemmas 2, 3 and 4 respectively.

Proof: From the definition of coverage probability,

$$\begin{aligned} P_{c_2}^{(\mathcal{Y})} &= \mathbb{E}_{R_1, R_2, \Theta} [\mathbb{P}(\text{SIR} > T | r_1, r_2, \theta)] = \mathbb{E}_{R_1, R_2, \Theta} [P(hr_2^{-\alpha} > T(I_1 + I_2 + I_3) | r_1, r_2, \theta)] \\ &\stackrel{(a)}{=} \mathbb{E}_{R_1, R_2, \Theta} [\mathbb{E}[e^{-s(I_1 + I_2 + I_3)} | r_1, r_2, \theta]] \\ &\stackrel{(b)}{=} \int_0^\infty \int_{z_1}^\infty \int_0^\pi \mathbb{E}[e^{-sI_1} | r_1, \theta] \mathbb{E}[e^{-sI_2} | r_1] \mathbb{E}[e^{-sI_3} | r_1, r_2] f_{R_2|R_1}(r_2 | r_1) f_{R_1}(r_1) f_\Theta(\theta) d\theta dr_2 dr_1 \end{aligned}$$

where (a) results from $h \sim \exp(1)$ and defining $s = Tr_2^\alpha$. Step (b) follows from the independence of the three interference powers and deconditioning w.r.t. R_1 , R_2 and Θ , where Θ is a uniform random variable in $[0, \pi]$ i.e. $f_\Theta(\theta) = 1/\pi$. From (2), (3) and (4), it can be seen that while I_1 and I_2 depend on just r_1 , I_3 is a function of both r_1 and r_2 . The result now follows by using the definition of Laplace transform for the interference powers and conditioning them accordingly. ■

The Laplace transform of the distribution of interference I_1 from a *singleton* is dealt first in the following Lemma.

Lemma 2. *Given v , the conditional Laplace transform of interference I_1 from a singleton defined in (2) is*

$$\mathcal{L}_{I_1|R_1, \Theta}(s | r_1, \theta) = 1 - q + \frac{q}{1 + s(r_1^2 + v^2 - 2r_1v \cos \theta)^{\frac{-\alpha}{2}}}.$$

Proof: By definition, the Laplace transform of interference is

$$\mathcal{L}_{I_1|R_1, \Theta}(s | r_1, \theta) = \mathbb{E}[e^{-st_x h_x r_{12}^{-\alpha}}] \stackrel{(a)}{=} 1 - q + q \mathbb{E}[e^{-sh_x r_{12}^{-\alpha}}] \stackrel{(b)}{=} 1 - q + \frac{q}{1 + sr_{12}^{-\alpha}},$$

where (a) follows from the fact that the interferer $x \in \Phi_B$ located at r_{12} is active with a probability q , and (b) results from $h_x \sim \exp(1)$. The final result follows by using the law of cosines in which $r_{12}^2 = r_1^2 + v^2 - 2r_1v \cos \theta$ (see Fig. 1). ■

The conditional Laplace transform of interference I_2 is derived next with its proof provided in Appendix A. The key is in handling the asymmetric exclusion zone \mathcal{C}_1 carefully. Interested readers can refer to [12] for more details on how such exclusion zones can be handled.

Lemma 3. *Given v , the conditional Laplace transform of I_2 under subcase \mathcal{Y} defined in (3) is*

$$\mathcal{L}_{I_2|R_1}(s|r_1) = \exp \left(-2p_B q \lambda \left(\int_{z_1}^{\infty} \frac{\pi r \, dr}{1 + \frac{r^\alpha}{s}} - \int_{|v-r_1|}^{v+r_1} \frac{f(r, r_1) r \, dr}{1 + \frac{r^\alpha}{s}} \right) \right),$$

$$\text{where } z_1 = \max(0, r_1 - v), f(r, r_1) = \cos^{-1} \left(\frac{r^2 + v^2 - r_1^2}{2rv} \right).$$

The conditional Laplace transform of interference I_3 is computed similarly with its proof provided in Appendix B.

Lemma 4. *Given v , the conditional Laplace transform of I_3 under subcase \mathcal{Y} is given by*

$$\mathcal{L}_{I_3|R_1, R_2}(s|r_1, r_2) = \exp \left(-p_A q \lambda \int_{r_2}^{\infty} \frac{2\pi r \, dr}{1 + \frac{r^\alpha}{s}} \right) \exp \left(p_A q \lambda \mathcal{B}(r_1, r_2, v) \right), \quad (5)$$

where $\mathcal{B}(r_1, r_2, v)$ is given by (9)

It is to be noted that the coverage probability analysis for a moving user conducted in this work is a generalization of the work in [4] for a static user ($v = 0$). Using the above results, we can also study the asymptotic coverage probability of file 2 when locations 1 and 2 are far apart ($v \rightarrow \infty$). In this case, $I_1 \rightarrow 0$, and the asymmetric exclusion zone \mathcal{C}_1 does not appear in I_2 and I_3 . The final result is given below.

Corollary 1. *For large user mobility ($v \rightarrow \infty$), the asymptotic coverage probability of file 2 is given by:*

$$P_{c_2} \rightarrow p_A \mathbf{P}_c(p_B) + p_B \mathbf{P}_c(p_A), \quad (6)$$

$$\text{where } \mathbf{P}_c(p) = \frac{p}{p + q[\rho_1(T, \alpha) + (1 - p)\rho_2(T, \alpha)]}, \quad (7)$$

$$\rho_1(T, \alpha) = T^{\frac{2}{\alpha}} \int_{T^{-\frac{2}{\alpha}}}^{\infty} \frac{du}{1 + u^{\frac{\alpha}{2}}}, \quad \rho_2(T, \alpha) = T^{\frac{2}{\alpha}} \int_0^{T^{-\frac{2}{\alpha}}} \frac{du}{1 + u^{\frac{\alpha}{2}}}. \quad (8)$$

Proof: For subcase \mathcal{Y} and $v \rightarrow \infty$, $\mathcal{L}_{I_1|R_1, \Theta}(Tr_2^\alpha|r_1, \theta) = 1$, $\mathcal{L}_{I_2|R_1}(Tr_2^\alpha|r_1) = \exp \left(-2\pi p_B q \lambda \int_0^{\infty} \frac{r \, dr}{1 + \frac{r^\alpha}{Tr_2^\alpha}} \right)$ and $\mathcal{L}_{I_3|R_1, R_2}(Tr_2^\alpha|r_1, r_2) = \exp \left(-2\pi p_A q \lambda \int_{r_2}^{\infty} \frac{r \, dr}{1 + \frac{r^\alpha}{Tr_2^\alpha}} \right)$. Also $v \rightarrow \infty$ corresponds to case 1 (disjoint circles) defined in our setup and thus $f_{R_2|R_1}(r_2|r_1) = 2p_A \lambda \pi r_2 \exp(-p_A \lambda \pi r_2^2)$ (from Lemma 1). Plugging the above values in Theorem 1 and defining $\rho_1(T, \alpha)$ and $\rho_2(T, \alpha)$

as in (8), we obtain $P_{c_2}^{(\mathcal{Y})} = P_c(p_A)$. Similarly, it can be shown that $P_{c_2}^{(\mathcal{X})} = P_c(p_B)$ for $v \rightarrow \infty$. The final result follows by applying total probability theorem to the two subcases \mathcal{X} and \mathcal{Y} . ■

C. “Local delay” at location 2

The average delay (also called *local delay*) [5] is defined as the mean number of time slots required by the transmitter to successfully transmit a packet to the receiver. Proceeding similar to the coverage probability analysis, the local delay in communicating with the closest device cached with file 2 for the typical user at location 2 is derived by applying total probability theorem to the two subcases \mathcal{X} and \mathcal{Y} as $D_2 = pD_2^{(\mathcal{X})} + (1 - p)D_2^{(\mathcal{Y})}$. Here $D_2^{(\mathcal{X})}$ and $D_2^{(\mathcal{Y})}$ denote the average delay of obtaining file 2 in subcases \mathcal{X} and \mathcal{Y} , respectively. Again, we focus only on subcase \mathcal{Y} as subcase \mathcal{X} can be handled by swapping the variables.

Conditioned on R_1 , R_2 , Θ and Φ , denote \mathcal{S} as the *success* event that the user at location 2 is successfully connected to the closest device cached with file 2 under subcase \mathcal{Y} . For an SIR threshold T , the conditional success probability is hence denoted as $P(\mathcal{S}) = \mathbb{P}(\text{SIR} > T | r_1, r_2, \theta, \Phi)$. If the user fails to decode the file, it is retransmitted in the next scheduled transmission slot. Accordingly, the number of time slots needed until success for a given R_1 , R_2 , Θ and Φ is a geometrically distributed random variable with mean $P(\mathcal{S})^{-1}$. Taking the expectation with respect to R_1 , R_2 , Θ and Φ yields the local delay of file 2 under subcase \mathcal{Y} :

$$\begin{aligned}
D_2^{(\mathcal{Y})} &= \mathbb{E}_{R_1, R_2, \Theta, \Phi} \left[\frac{1}{\mathbb{P}(\text{SIR} > T | r_1, r_2, \theta, \Phi)} \right] \\
&= \mathbb{E}_{R_1, R_2, \Theta, \Phi} \left[\frac{1}{P(h > Tr_2^\alpha (I_1 + I_2 + I_3) | r_1, r_2, \theta, \Phi)} \right] \\
&\stackrel{(a)}{=} \mathbb{E}_{R_1, R_2, \Theta, \Phi} \left[\frac{1}{\mathbb{E}[e^{-sI_1} | r_1, \theta, \Phi] \mathbb{E}[e^{-sI_2} | r_1, \Phi] \mathbb{E}[e^{-sI_3} | r_1, r_2, \Phi]} \right] \\
&\stackrel{(b)}{=} \int_0^\infty \int_{z_1}^\infty \int_0^\pi \underbrace{\mathbb{E}_\Phi \left[\frac{1}{\mathcal{L}_{I_1|R_1, \Theta}(s | r_1, \theta, \Phi)} \right]}_{D_{I_1}} \underbrace{\mathbb{E}_\Phi \left[\frac{1}{\mathcal{L}_{I_2|R_1}(s | r_1, \Phi)} \right]}_{D_{I_2}} \\
&\quad \underbrace{\mathbb{E}_\Phi \left[\frac{1}{\mathcal{L}_{I_3|R_1, R_2}(s | r_1, r_2, \Phi)} \right]}_{D_{I_3}} f_{R_2|R_1}(r_2 | r_1) f_{R_1}(r_1) f_\Theta(\theta) d\theta dr_2 dr_1
\end{aligned}$$

where (a) results from $h \sim \exp(1)$ and defining $s = Tr_2^\alpha$. (b) follows from the independence of the three interference powers (I_1 , I_2 and I_3) and deconditioning w.r.t. R_1 , R_2 and Θ . The final

result for the local delay of obtaining file 2 in subcase \mathcal{Y} is now presented in the next Theorem with the details of the rest of the steps provided in Appendix C.

Theorem 2. *The local delay of obtaining file 2 at location 2 in a PPP of intensity λ for subcase \mathcal{Y} is*

$$D_2^{(\mathcal{Y})} = \int_0^\infty \int_{z_1}^\infty \int_0^\pi D_{I_1} D_{I_2} D_{I_3} f_{R_2|R_1}(r_2|r_1) f_{R_1}(r_1) f_\Theta(\theta) d\theta dr_2 dr_1$$

$$\text{where } D_{I_1} = \left(1 - q + \frac{q}{1 + s(r_1^2 + v^2 - 2r_1v \cos \theta)^{-\alpha/2}} \right)^{-1},$$

$$D_{I_2} = \exp \left(2p_B q \lambda \left(\int_{z_1}^\infty \frac{\pi r dr}{1 - q + \frac{r^\alpha}{s}} - \int_{|v-r_1|}^{v+r_1} \frac{f(r, r_1) r dr}{1 - q + \frac{r^\alpha}{s}} \right) \right) \text{ and}$$

$$D_{I_3} = \exp \left(p_A q \lambda \int_{r_2}^\infty \frac{2\pi r dr}{1 - q + \frac{r^\alpha}{s}} \right) \exp \left(-p_A q \lambda \mathcal{B}_1(r_1, r_2, v) \right).$$

where $f(r, r_1)$ is defined in Lemma 3 and $\mathcal{B}_1(r_1, r_2, v)$ given by (10).

IV. RESULTS AND DISCUSSION

Fig. 2 plots the coverage probability and average delay of file 2 for various levels of mobility in a 2-file distributed caching system. As evident from the figure, mobility increases the coverage probability of obtaining the farther cached file portion (file 2). For a static user, the low coverage of file 2 is due to the presence of a dominant interferer (file 1) located closer to the user than the serving device (file 2). With user mobility, the likelihood of having a dominant interferer that is located closer to the serving device reduces, which improves the coverage of file 2. The above observation also explains the lower delay values encountered with user mobility as shown in Fig. 2 (*right*). Also, it can be observed that coverage probability decreases with activity factor; the corresponding plots are not shown here due to the lack of space.

V. CONCLUSION

The effect of mobility on the coverage probability and average delay of the farther cached file portion in a 2-file distributed caching D2D network is studied in this paper. The novelty lies in the *exact* mobility-aware analysis that has to capture the information of the local neighborhood of nodes at the original location of the device. Our analysis concretely shows that user mobility

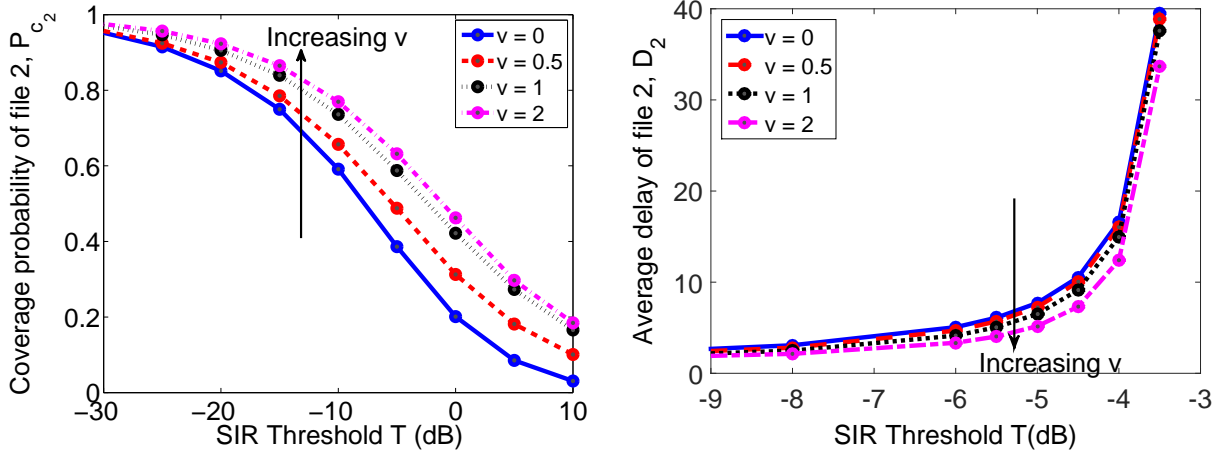


Fig. 2. Effect of mobility v on the coverage probability and average delay of file 2 ($p_A = 0.5, q = 0.5, \alpha = 4, \lambda = 1$).

improves this coverage probability and average delay in a uniform caching network. This improvement is a result of lower likelihood of having dominant interferer closer than the serving device.

APPENDIX

A. Proof of Lemma 3

The conditional Laplace transform of interference I_2 (all file B devices except the *singleton*) is written as

$$\begin{aligned}
 \mathcal{L}_{I_2|R_1}(s|r_1) &= \mathbb{E} \left[\exp \left(-s \sum_{y \in \Phi_B \setminus \mathcal{C}_1} t_y h_y \|y\|^{-\alpha} \right) \right] \stackrel{(a)}{=} \mathbb{E} \left[\prod_{y \in \Phi_B \setminus \mathcal{C}_1} 1 - q + \frac{q}{1 + s \|y\|^{-\alpha}} \right] \\
 &\stackrel{(b)}{=} \exp \left(-p_B q \lambda \int_{\mathbb{R}^2 \setminus (\mathcal{C}_3 \cup (\mathcal{C}_1 \setminus \mathcal{C}_3))} \frac{dy}{1 + \frac{\|y\|^\alpha}{s}} \right) \\
 &\stackrel{(c)}{=} \exp \left(-p_B q \lambda \left(\int_{\mathbb{R}^2 \setminus \mathcal{C}_3} \frac{dy}{1 + \frac{\|y\|^\alpha}{s}} - \int_{\mathcal{C}_1 \setminus \mathcal{C}_3} \frac{dy}{1 + \frac{\|y\|^\alpha}{s}} \right) \right) \\
 &\stackrel{(d)}{=} \exp \left(-p_B q \lambda \left(\int_{z_1}^{\infty} \frac{2\pi r dr}{1 + \frac{r^\alpha}{s}} - \int_{|v-r_1|}^{v+r_1} \frac{2 \cos^{-1} \left(\frac{r^2 + v^2 - r_1^2}{2rv} \right) r dr}{1 + \frac{r^\alpha}{s}} \right) \right)
 \end{aligned}$$

where (a) follows from $h_y \sim \exp(1)$ while considering the activity factor q of the interferers, (b) results from the PGFL of the PPP Φ_B and expressing \mathcal{C}_1 as the union of \mathcal{C}_3 and $\mathcal{C}_1 \setminus \mathcal{C}_3$, where

$\mathcal{C}_3 = \mathbf{b}(0, z_1)$ and $z_1 = \max(0, r_1 - v)$ (See Fig. 1), and (c) follows by splitting the integral into the two regions. Further, we obtain (d) by converting the integral from Cartesian to polar coordinates and using the law of cosines in which $r^2 + v^2 - 2rv \cos \gamma = r_1^2$ (see Fig. 1). The lower limit of the integration region of $\mathcal{C}_1 \setminus \mathcal{C}_3$ (dark shaded region in Fig. 1) takes values of $r_1 - v$ and $v - r_1$ for scenarios 1 and 2 respectively, therefore we use the absolute value $|v - r_1|$ as the lower limit to capture both scenarios.

B. Proof of Lemma 4

Proceeding similar to (a) in Appendix A, the conditional Laplace transform of I_3 , $\mathcal{L}_{I_3|R_1, R_2}(s|r_1, r_2)$

$$\begin{aligned}
&= \mathbb{E} \left[\prod_{z \in \Phi_A \setminus (\mathcal{C}_1 \cup \mathcal{C}_2)} 1 - q + \frac{q}{1 + s \|z\|^{-\alpha}} \right] \\
&\stackrel{(a)}{=} \exp \left(-p_A q \lambda \left(\int_{\mathbb{R}^2 \setminus \mathcal{C}_2} \frac{dz}{1 + \frac{\|z\|^\alpha}{s}} - \int_{\mathcal{C}_1 \setminus \mathcal{C}_2} \frac{dz}{1 + \frac{\|z\|^\alpha}{s}} \right) \right) \\
&\stackrel{(b)}{=} \exp \left(-p_A q \lambda \int_{r_2}^{\infty} \frac{2\pi r dr}{1 + \frac{r^\alpha}{s}} \right) \exp \left(p_A q \lambda \underbrace{\int_{\mathcal{C}_1 \setminus \mathcal{C}_2} \frac{2f(r, r_1) r dr}{1 + \frac{r^\alpha}{s}}}_{\mathcal{B}(r_1, r_2, v)} \right)
\end{aligned}$$

where (a) results from the PGFL of the PPP Φ_A and splitting the integral into two regions, (b) follows by converting the integral from Cartesian to polar coordinates and using the law of cosines with $f(r, r_1)$ defined in Lemma 3. The integral in the second term of (b) depends on the integration region $\mathcal{C}_1 \setminus \mathcal{C}_2$ with its lower limit (denoted by a in Fig. 1) taking values $\{v - r_1, r_2\}$ for cases 1 and 2. The integration region is zero for case 3 as $\mathcal{C}_1 \setminus \mathcal{C}_2 = \emptyset$ (\mathcal{C}_1 is engulfed inside \mathcal{C}_2). The integral $\mathcal{B}(r_1, r_2, v)$ is summarized below.

$$\mathcal{B}(r_1, r_2, v) = \begin{cases} \int_{v-r_1}^{v+r_1} \frac{2f(r, r_1) r dr}{1 + \frac{r^\alpha}{s}}, & \text{case 1} \\ \int_{r_2}^{v+r_1} \frac{2f(r, r_1) r dr}{1 + \frac{r^\alpha}{s}}, & \text{case 2} \\ 0, & \text{case 3} \end{cases} \quad (9)$$

C. Proof of Theorem 2

Conditioned on R_1 , R_2 and Θ , the local delay of obtaining file 2 is dictated by the local delay from three interference regions individually (D_{I_1} , D_{I_2} and D_{I_3}). By definition

$$\begin{aligned}
D_{I_1} &\stackrel{(a)}{=} \mathbb{E}_\Phi \left[\frac{1}{1 - q + q\mathbb{E}[e^{-sh_x r_{12}^{-\alpha}}]} \right] \stackrel{(b)}{=} \frac{1}{1 - q + \frac{q}{1 + sr_{12}^{-\alpha}}} \\
D_{I_2} &= \mathbb{E}_\Phi \left[\frac{1}{\mathcal{L}_{I_2|R_1}(s|r_1, \Phi)} \right] \stackrel{(c)}{=} \mathbb{E}_\Phi \left[\prod_{y \in \Phi_B \setminus \mathcal{C}_1} \frac{1}{1 - q + q\mathbb{E}[e^{-sh_y \|y\|^{-\alpha}}]} \right] \\
&\stackrel{(d)}{=} \exp \left(-2\pi p_B \lambda \int_{\mathbb{R}^2 \setminus (\mathcal{C}_3 \cup (\mathcal{C}_1 \setminus \mathcal{C}_3))} \left(1 - \frac{1}{1 - q + \frac{q}{1 + sr^{-\alpha}}} \right) r \, dr \right) \\
D_{I_3} &\stackrel{(e)}{=} \mathbb{E}_\Phi \left[\prod_{z \in \Phi_A \setminus (\mathcal{C}_1 \cup \mathcal{C}_2)} \frac{1}{1 - q + q\mathbb{E}[e^{-sh_z \|z\|^{-\alpha}}]} \right] \\
&\stackrel{(f)}{=} \exp \left(p_A q \lambda \int_{r_2}^{\infty} \frac{2\pi r \, dr}{1 - q + \frac{r^\alpha}{s}} \right) \exp \left(-p_A q \lambda \mathcal{B}_1(r_1, r_2, v) \right), \\
\text{where } \mathcal{B}_1(r_1, r_2, v) &= \begin{cases} \int_{v-r_1}^{v+r_1} \frac{2f(r, r_1) r \, dr}{1 - q + \frac{r^\alpha}{s}}, & \text{case 1} \\ \int_{r_2}^{v+r_1} \frac{2f(r, r_1) r \, dr}{1 - q + \frac{r^\alpha}{s}}, & \text{case 2} \\ 0, & \text{case 3} \end{cases} \quad (10)
\end{aligned}$$

where (a) follows by considering the activity factor q of the interferers, (b) results from $h_x \sim \exp(1)$ and the final expression of D_{I_1} obtained by using $r_{12}^2 = r_1^2 + v^2 - 2r_1 v \cos \theta$. Proceeding similar to (a) and (b), we obtain (c) while (d) results from the PGFL of the PPP Φ_B and converting the integral from Cartesian to polar coordinates. The final expression of D_{I_2} is obtained by proceeding similar to the last step in Appendix A. Steps (e) and (f) follow by proceeding similar to Appendix B.

REFERENCES

- [1] N. Golrezaei, A. F. Molisch, A. G. Dimakis, and G. Caire, "Femtocaching and device-to-device collaboration: A new architecture for wireless video distribution," *IEEE Communications Magazine*, vol. 51, no. 4, pp. 142–149, April 2013.
- [2] E. Altman, K. Avrachenkov, and J. Goseling, "Distributed storage in the plane," in *Proc. IFIP Networking Conference*, 2014.
- [3] N. Golrezaei, A. G. Dimakis, and A. F. Molisch, "Wireless device-to-device communications with distributed caching," in *Proc. IEEE ISIT*, Cambridge, MA, July 2012.
- [4] S. Krishnan and H. S. Dhillon, "Distributed caching in device-to-device networks: A stochastic geometry perspective," in *Proc. Asilomar*, Nov 2015.
- [5] Z. Gong and M. Haenggi, "The local delay in mobile poisson networks," *IEEE Transactions on Wireless Communications*, vol. 12, no. 9, pp. 4766–4777, September 2013.

- [6] S. K. Dandapat, S. Pradhan, N. Ganguly, and R. Roy Choudhury, “Sprinkler: Distributed content storage for just-in-time streaming,” in *Proc. ACM Workshop on Cellular Networks: Operations, Challenges, and Future Design (CellNet’13)*, Jun 2013.
- [7] K. Poularakis and L. Tassiulas, “Exploiting user mobility for wireless content delivery,” in *Proc. IEEE ISIT*, Istanbul, Turkey, July 2013.
- [8] X. Lin, R. Ratasuk, A. Ghosh, and J. G. Andrews, “Modeling, analysis, and optimization of multicast device-to-device transmissions,” *IEEE Transactions on Wireless Communications*, vol. 13, no. 8, pp. 4346–4359, Aug 2014.
- [9] Z. Han and K. J. R. Liu, *Resource Allocation for Wireless Networks: Basics, Techniques, and Applications*. Cambridge, U.K.: Cambridge University Press, 2008.
- [10] M. Haenggi, *Stochastic Geometry for Wireless Networks*. New York: Cambridge University Press, 2013.
- [11] J. G. Andrews, F. Baccelli, and R. K. Ganti, “A tractable approach to coverage and rate in cellular networks,” *IEEE Trans. Commun.*, vol. 59, no. 11, pp. 3122–3134, 2011.
- [12] Z. Yazdanshenasan, H. S. Dhillon, M. Afshang, and P. H. J. Chong, “Poisson hole process: Theory and applications to wireless networks,” submitted to *IEEE Trans. on Wireless Commun.*, 2015, available online: <http://arxiv.org/abs/1601.01090>.